



This open access document is published as a preprint in the Beilstein Archives with doi: 10.3762/bxiv.2019.133.v1 and is considered to be an early communication for feedback before peer review. Before citing this document, please check if a final, peer-reviewed version has been published in the Beilstein Journal of Nanotechnology.

This document is not formatted, has not undergone copyediting or typesetting, and may contain errors, unsubstantiated scientific claims or preliminary data.

Preprint Title Hydrogen Sulfide Removal Using Various Metal Oxide Nanocomposite from Drilling Fluid: Optimization, Kinetic and Adsorption Isotherms

Authors Mohamad M. Nemati, Rahmatallah Saboori and Samad Sabbaghi

Publication Date 28 Okt 2019

Article Type Full Research Paper

ORCID® IDs Samad Sabbaghi - <https://orcid.org/0000-0003-4689-4081>

Hydrogen Sulfide Removal Using Various Metal Oxide Nanocomposite from Drilling Fluid: Optimization, Kinetic and Adsorption Isotherms

Mohamad Mehdi Nemati¹, Rahmatallah Saboori², Samad Sabbaghi^{1,*}

¹Dep. of Nano-Chemical Eng., Faculty of advanced technologies, Shiraz University

²Drilling Nano Fluid Lab., Faculty of advanced technologies, Shiraz University

Abstract

In a drilling operation, the existing hydrogen sulfide in oil and gas reservoirs can be solved in drilling fluid and cause some environmental problems and life-threatening situations to personnel. Therefore, hydrogen sulfide removal of drilling fluid is so important. In this work, in order to hydrogen sulfide removal from drilling fluid, zinc oxide nanoparticle, silica nanoparticle and silica/zinc oxide nanocomposite with different ratio were synthesized by precipitation and sol-gel method and characterized by x-ray diffraction, fourier-transform infrared spectroscopy, Field emission scanning electron microscopy, energy dispersive x-ray and brunauer–emmett–teller. The Design Expert software, I-optimal, was used to design the experiments and the optimum condition for hydrogen sulfide removal was determined. Also, the effect of nanomaterial concentration, hydrogen sulfide concentration, contact time, pH and type of nanomaterial on removal of hydrogen sulfide was investigated. the results show, the optimization of removal at nanoparticle concentration, 0.1 and 0.9 wt.%, hydrogen sulfide concentration, 800 ppm, contact time, 3 min., pH, 12 and ZnO/SiO₂ nanocomposite with 3:1 ratio is about 92.6 and 97.2%. investigation of the reaction kinetic showed that hydrogen sulfide removal had a very high rate, so that time parameter has a low impact on the removal process. Also, the kinetic adsorption was pseudo-first order. Adsorption of hydrogen sulfide followed Freundlich isotherm model and multilayer adsorption. The reusability of nanocomposite is four cycles for hydrogen sulfide removal more than 50%, which was significant in industrial processes.

Keywords: Hydrogen sulfide, Removal, Drilling fluid, Nanoparticle, Nanocomposite, Zinc oxide/Silica.

*Phone: +989171133471; Fax: +9871-36139669; E-mail: sabbaghi@shirazu.ac.ir.

*Phone: +15195699734; E-mail: samad.sabbaghi@uwaterloo.ca & s2sabbagh@uwaterloo.ca.

1. Introduction

One of the most important and the most expensive part of drilling of oil and gas well is drilling fluid. Drilling fluid has an essential role in oil and gas wells drilling that do the task of carrying cuttings to the surface, cooling and lubricating the bit, cleaning the bottom hole and etc. These properties are emerged by adding additives into the fluid (Saboori et al. 2018; Dargahi-Zaboli et al. 2017). Some problems may happen during the drilling operation which the significant one is the presence of sulfur compounds like H_2S , HS^- and S^{2-} that enters from well formation to drilling fluid (Sunde and Olsen 1999). These sulfur compounds are very dangerous and deadly to personnel, corrosion and cracking of drill pipe and causing environmental pollution (Carney and Jones 1974). The limit for this pollutant in different parts of oil and gas industry should be less than 8ppm. There are varied methods to removal of hydrogen sulfide, that one of the most important method is chemical and physical adsorption. Carney et al. described the history of proceeding that used against destructive effects of dihydrogen sulfide gases in drilling fluid. In order to reduce the effects of hydrogen sulfide, they suggested the use of materials such as copper, zinc, iron, chelates, and hydrogen peroxide. It is noteworthy that, these compounds were suitable for use in water base drilling fluids (Carney and Jones 1974).

But, in a recent year, nanomaterial as an additive are employed to improve of rheology and adsorb of pollutant from drilling fluid. It is noteworthy that, the drilling fluid rheology should not get damaged by adding nanomaterial as adsorbents. Awume et al. used zinc oxide nanoparticle for hydrogen sulfide removal from low temperature gas and the effect of gas flow rate, H_2S concentration, particle size, temperature on removal was investigated. Their results showed the with increases in hydrogen sulfide concentration and temperature and with decreases in particle size and gas flow rate led to increase adsorption (Awume et al. 2017). Daneshyar et al. modified carbon active by copper, zinc and nickel cobalt and nickel nanoparticles and γ -alumina by cobalt and nickel nanoparticles as an adsorbent of hydrogen sulfide. Also, the effect of adsorbent concentration, flow rate, temperature, pressure and amount of gas on hydrogen sulfide removal were investigated and determined optimum condition. Their results indicated, maximum removal of hydrogen sulfide at optimum condition were 94% and 91.6% for Cu-Zn-Ni/active carbon and Co-Ni/ γ -alumina at optimum condition (Daneshyar et al. 2017). Salehi Morgani et al. experimentally investigated the effect of synthesized metal oxide and ZnO/TiO₂ nanocomposite on hydrogen sulfide from drilling fluid. Their indicated ZnO, TiO₂ and ZnO/TiO₂ nanocomposite decreased hydrogen sulfide in drilling fluid from 800 ppm to about 250, about 150 and less than 5 ppm at 10 min. and 0.67 wt% of nanomaterial (Morgani et al. 2017). Liu et al. investigated

the effect of hybrid adsorbent/photocatalytic composite of coated zeolite by TiO_2 (various TiO_2 concentration) on selective removal hydrogen sulfide from biogas. They demonstrated the composite with 5wt.% of TiO_2 was the highest removal of hydrogen sulfide capacity (0.13 mmol/g) compare with zeolite (0.05 mmol/g) and TiO_2 nanoparticle (0.07 mmol/g) (Liu et al. 2015). Fauteux-Lefebvre et al. synthesized functionalization of carbon nanofilament by iron nanoparticle and its impact was studied on adsorption of hydrogen sulfide that exist in depths. They indicated that this adsorbent has ability to decrease hydrogen sulfide concentration from 500 to below 1.5 ppm at 20 wt/wt.% metal loading. Also, temperature is an important parameter in adsorption of hydrogen sulfide gases (Fauteux-Lefebvre et al. 2015). Blatt et al. prepared iron oxide/ polymer based nanocomposite and used for adsorption of hydrogen sulfide. Their experiments indicated this adsorbent is higher capacity for adsorption of hydrogen sulfide (Blatt et al. 2014). Wang et al. synthesized mesoporous silica SBA-15 supported Zinc oxide nanoparticle (different loading) and investigated its effect on removal of hydrogen sulfide from gas. Their results showed this nanoparticle with the highest breakthrough capacity, 436 mg S/ g adsorbent, removed hydrogen sulfide from gas 0.1 vol.% to below 0.1 ppb at 39 min, room temperature, 3.04 wt.% Zn loading (Wang et al. 2008). Zhang et al. reported removal of hydrogen sulfide from hot coal gas by different mesoporous silica supported by Mn_2O_3 (Zhang et al. 2014). Esmaeili-Faraj et al. studied adsorption of hydrogen sulfide and carbone dioxide by Graphene Oxide and silica in water based nanofluid (Esmaeili-Faraj et al. 2016). Ma et al. used SiC nanoparticles for removal hydrogen sulfide from natural gas by traditional desulfurizer (Ma et al. 2017). Also, Sekhvatjou et al used iron and zinc oxide for removal sulfur component (hydrogen sulfide, carbonyl sulfide, methyl mercaptan, ethyl mercaptan, dimethyl sulfide, and carbon disulfide) from sour gas (Sekhvatjou et al 2014).

The most nanomaterials used to remove hydrogen sulfide are nanoparticles and rarely use of nanocomposite has been reported. It is noteworthy that, zinc oxide and silica nanoparticles are widely used in drilling fluid. In this work, zinc oxide nanoparticle, silica nanoparticle and zinc oxide/silica nanocomposite with different ratio were synthesized and characterized. Then, synthesized nanomaterial added to drilling fluid and amount of removal hydrogen sulfide was studied. in order to design of experiment and determination of optimum condition for removal of hydrogen sulfide, Design expert software was used. Finally, kinetic and isotherm study of hydrogen sulfide adsorption, and resiability of synthesized nanomaterial were investigated.

2. Materials and method

2.1. Materials

Zinc acetate dihydrate ($\text{Zn}(\text{CH}_3\text{COO})_2 \cdot 2\text{H}_2\text{O}$), tetraethyl orthosilicate ($\text{SiC}_8\text{H}_{20}\text{O}_4$), ethanol (CH_2COOH), nitric acid (HNO_3), sodium hydroxide (NaOH), sodium sulfide hydrate (Na_2S), and acid chloric (HCl) were purchased from Merck company. Deionized water was purchased from Zolal company, and sodium bentonite was provided from Iranian National Drilling Company.

2.2. Synthesis of nanomaterial

2.2.1. Zinc oxide nanoparticle

Zinc oxide (ZnO) nanoparticles were synthesized by precipitation method (Kumar et al. 2013; Hasnidawani et al. 2016). which is one of the useful, simple, and inexpensive methods to produce nanoparticles. For this work, zinc acetate dihydrate (2gr) was added to distilled water (15 ml) and mixed by vigorous magnetic stirrer. Then, sodium hydroxide (2M, 10 ml) added to the solution and mixed by magnetic stirrer at room temperature for 10 min., Ethanol (100 ml) was added gradually to final solution with magnetic stirrer. The color solution was changed to white and precipitate obtained. This with precipitate was including ZnO nanoparticles and sodium acetate salt. In order to purify and separate the ZnO nanoparticle from sodium acetate, the precipitate was washed for several times with distilled water and ethanol. Finally, the sediments were dried in 80°C for 2 hr.

2.2.2. Silica nanoparticle

In order to produce silica (SiO_2) nanoparticle with sol-gel method (Rahman and Padavettan 2012; Saboori et al. 2018), ethanol and tetraethyl orthosilicate with a volume ratio of 1:5 was mixed by magnetic stirrer (solution A). Then ammonia solution was added to distilled water with volume ratio of 1:1 (solution B). Solution A and B were mixed for 10 min at room temperature. After 20 min., sol (milky color) and gel were formed. The gel was dried in room temperature. Finally, the obtained powder was calcined for 1 hr in 600°C .

2.2.3. Silica/zinc oxide nanocomposite

Zinc oxide/silica (ZnO/SiO_2) nanocomposite was produced by sol-gel method. Two solutions were prepared to the synthesis of silica/zinc oxide nanocomposite. The first solution contained zinc acetate dihydrate, deionized water, and nitric acid. For preparation of this solution, zinc acetate dihydrate was added to deionized water and the pH of solution was set on 4 with nitric acid. The second solution contained ethanol and tetraethyl orthosilicate, which was stirred by magnetic stirrer for 10 min., at room temperature. The second solution was added dropwise to the first

solution. and stirred for 2 hr by magnetic stirrer. After 30 min., the sol and gel was formed. Finally, the gel was dried in room temperature and finally, the powder was calcined at 300 °C for 1hr. Fig. 1 shows the procedure of ZnO/SiO₂ nanocomposite synthesis with a ratio of 1:1. It is noteworthy that, the nanocomposite with another ratio, 3:1 and 1:3, were synthesized by this method. Also, Table 1 shows the amount of material for synthesis of nanocomposite with a different ratio.

Fig. 1

Table 1

2.3. Preparation of drilling fluid and hydrogen sulfide removal

In order to investigate the removal of hydrogen sulfide from water based drilling fluid with ZnO and SiO₂ nanoparticles and SiO₂/ZnO nanocomposite, 10 gr of bentonite and 350 ml of deionized water were mixed by Hamilton Batch Mixer with 36000 rpm for 20 min (as a water based drilling fluid). The certain amount of sodium sulfide hydrate was added to drilling fluid and mixed by Hamilton Batch mixer for 15 min. Then synthesized nanoparticle and nanocomposite with certain concentration was added to the mixture for certain contact time. The mixture was filtrate and centrifuge. Finally, removal of hydrogen sulfide in drilling fluid was measured by UV-visible spectrophotometer. It is noteworthy that, the effect of nanomaterial concentration, hydrogen sulfide concentration, contact time, pH and type of nanocomposite was investigated in the removal of hydrogen sulfide. In order to investigate the effect of parameter and interaction between this parameter was used Design Expert software (trial 10, I-optimal method). One of the benefits of using Design Expert software is determining the effective parameters and the effect of this parameter on hydrogen sulfide removal, hence with the definition of p-value and F-value factors, the software determines effective variables and interaction between of parameters. Table 2 illustrates the parameter and their range on removal hydrogen sulfide from water based drilling fluid.

Table 2

2.4. Characterization

In order to characterize the synthesized nanoparticles and nanocomposite, x-ray diffraction (XRD), fourier transform infrared spectroscopy (FTIR), field emission scanning electron microscopy (FE-SEM), energy-dispersive x-ray spectroscopy (EDXA), and brunauer–emmett–teller (BET) were used. The XRD analysis is used to confirm the validity of the synthesized nanomaterial, specification of the amorphous or crystalline form of the produced particles

and crystal size of produced nanomaterial with the Scherrer equation. The FT-IR analysis is also for validation of the produced substance and chemical bond determination between elements in a specimen. The nanocomposite proportion can be determined by EDAX analysis, which is an elemental analysis. Moreover, the FE-SEM image is used to specify the synthesized nanomaterial appearance shape. The specific surface area of the synthesized nanoparticles can be designated by BET analysis.

3.Results and discussion

3.1. Characterization of nanomaterial

- XRD

The XRD pattern of the synthesized ZnO and SiO₂ nanoparticles and ZnO/SiO₂ nanocomposite with the ratios of 1:1, 1:3 and 3:1 demonstrate in Fig. 2-a to b. In Fig. 2-a, It is obvious that the peaks of 2θ equal to 31.75°, 34.45°, 36.25°, 47.6°, 56.6°, 62.8°, 67.95°, and 69.2 ° are related to the plates of (100), (002), (101), (102), (110), (103), and (112) in the XRD spectrum, as for ZnO nanoparticle and indicates the validity of the synthesized nanoparticles (Lim et al. 2011; Bagheri et al. 2013; Hasnidawani et al. 2016). In Fig. 2-b, the peaks of equal to 2θ are related to the plates of 11.65°, 13.16°, 19.53°, 22.25°, in the XRD spectrum, as for silica nanoparticle (Ali et al. 2016; Goldstein et al. 2017).

The XRD analysis of ZnO/SiO₂ nanocomposite with a ratio of 1:1 is shown in Fig. 2-c. The peaks that are in 11.72°, 19.16°, 20.56°, 22.92°, 24.80°, 29.86° are related to the SiO₂ nanoparticle, and the peaks in 31°, 34.21°, 36.33°, 51.99°, 53.53°, 62.91° are dedicated to ZnO nanoparticle, which shows the presence of two nanoparticles in the synthesized nanocomposite (Stöber et al. 1968; Arshad et al. 2015). The peaks, in Fig. 2-d for ratio of 3:1, are in 2θ equal to 11.47°, 13.69°, 18.86°, 23.13°, 25.91°, 28.80°; and in Fig. 2-e for ratio of 1:3 are in 65.08°, 47.13°, 68.02°, 62° are indicating the validity of the synthesized nanocomposites, and are related to the plates of (103), (110), (020), (021), (101), (200), (130), (201) of SiO₂ nanoparticle in Fig. 2-d, and the plates of (020), (201), and (212) of silica in Fig. 2-e, respectively. Also, the 2θ equal to 31.75°, 34.42°, 36.31°, 39.86°, 47.56°, 51.01°, 56.70°, 64.10°, 100° in Fig. 2-d; and 31.86°, 34.33°, 36.32°, 56.70°, and 62.91° in Fig. 2-e are related to the plates of (002), (101), (102), (110), and (103) of ZnO nanoparticle in Fig. 2-e and d, respectively (Stöber et al. 1968; Han et al. 2006; Arshad et al. 2015).

Fig. 2

The crystallite size results of the synthesized nanoparticles and nanocomposites are obtained by Scherrer equation (Eq. 1) and provided in Table 3 (Speakman 2014).

$$\tau = \frac{K\lambda}{\beta \cos\theta} \quad (1)$$

Which in this equation τ (nm) is the average size of crystalline, K is shape factor, λ is x-ray source wavelength (0.154056 nm), β is the line broadening at half the maximum intensity height in radian, and θ is the Bragg angle (degree).

Table 3

- EDAX

Fig. 3 show the result of EDAX analysis of the synthesized ZnO/SiO₂ nanocomposite with 1:3, 1:1, and 3:1 ratio. In this Fig., the presence of Zn and Si in nanocomposite with different ratio indicate the validity of synthesized nanocomposite. So that 25.3 wt.% of Zn and 74.7 wt.% of Si, 47.1 wt.% of Zn and 52.9 wt.% of Si and 75.9 wt.% of Zn and 24.1 wt.% of Si confirm the synthesised nanocomposite with ratios of 1:3, 1:1 and 3:1, respectively.

Fig. 3

-FTIR

Fig. 4-a shows FTIR spectra of ZnO nanoparticles. The adsorption peaks at 2400 and 3500 cm⁻¹ are related to O-H bond. The peak at 575.12 cm⁻¹ is correspond to Zn-O band. The peaks which revealed at 418 cm⁻¹ and 1400-1600 cm⁻¹ are dedicated to O-H and Zn-O (Han et al. 2006; Jurablu et al. 2015). FTIR analysis of synthesized SiO₂ nanoparticle is shown in Fig. 4-b. The peak around 472.12 cm⁻¹ are corresponds to Si-O. The peaks of 820 and 1100 cm⁻¹ refer to Si-O-Si band. The oxygen and metal bond emerges at around 500 cm⁻¹ (Saboori et al. 2018). Therefore, the these peaks (see Fig. 4-a and b) confirms the validity of Synthesized ZnO and SiO₂ nanoparticle (Bagheri et al. 2013; Jurablu et al. 2015; Skoog et al. 2017).

The FTIR spectra of SiO₂/ZnO nanocomposite with different ratios are shown in Fig. 4-c. The peak at about 970 cm⁻¹ refer to Zn-O-Si bond which confirms the synthesized nanocomposite validity (Musić et al. 2011; Liu et al. 2012;

Shastri et al. 2013; Raevskaya et al. 2014). Also, another peak shows Si-O, Zn-O, Si-O-Si, O-H band on nanocomposite that emerge at all ratio of nanocomposite.

Fig. 4

-FE-SEM analysis

Fig. 5-a to e illustrates FE-SEM image of synthesized ZnO, SiO₂ nanoparticles and ZnO/SiO₂ nanocomposite with ratios of 1:1, 1:3, and 3:1. It is observed that ZnO nanoparticle has in plate-like shape, SiO₂ nanoparticle and nanocomposites in all ratios have in semispherical shape.

Fig. 5

- BET analysis

BET analysis is used in order to measure and compare specific surface area of nanomaterial. By increasing of the specific surface area, the active sites of nanomaterial for hydrogen sulfide removal increases, therefore the removal enhances. The result of BET analysis of synthesized nanoparticle and nanocomposite are shown in Table 4. It is obvious that the specific surface area of ZnO/SiO₂ nanocomposites is bigger than ZnO and SiO₂ nanoparticle. Also, the specific surface area of ZnO/SiO₂ nanocomposite with ratio of 1:3 is 208.82 m² gr⁻¹ that has the highest specific area among synthesized nanoparticles.

Table 4

3.2. Design of experiment and effective parameters in hydrogen sulfide removal

Generally, two types of variables are important in the software. The first types are qualitative variables that represent a variable kind and quality such as nanocomposite type that synthesize in three different ratios (1:3, 1:1, 3:1). The second types are quantitative variables that a range of variation defines for them. Effective quantitative variables on the removal hydrogen sulfide from drilling fluid are showed in Table 3. Design Expert software (trial 10, I-Optimal method), 42 experiments were designed, that list of experiments and their results show in Table 5. P-value and F-value for all main parameter and also effective parameter (interaction between parameter) are provided in Table 6. It is obvious that, the nanoparticle concentration, pH, and ratio of nanocomposite are the most effective on hydrogen sulfide removal and hydrogen sulfide concentration is more effective than contact time.

Table 5

Table 6

- Effect of main parameter

The most important factor in hydrogen sulfide removal from drilling fluid is nanoparticle concentration (F-value < 0.005). Fig. 6-a demonstrates the effect of nanoparticle concentration on hydrogen sulfide removal from drilling fluid at condition of hydrogen sulfide concentration=800 ppm, contact time=15 min, pH=10, and ratio of ZnO/SiO₂ nanocomposite= 3:1. Hydrogen sulfide in drilling fluid adsorbed on the nanoparticles and nanocomposites surfaces. So that, the increasing nanoparticle concentration are, the active site (surfaces area) for removal enhances, therefore the hydrogen sulfide removal from drilling fluid increase. By increasing of the nanoparticle concentration from 0.1 to 0.9 wt.%, the removal enhances from 93 to 98%.

The second influential quantitative variable in hydrogen sulfide removal is initial hydrogen sulfide concentration in drilling fluid. Fig. 6-b shows the effect of hydrogen sulfide concentration on removal of hydrogen sulfide from drilling fluid at condition of nanoparticle concentration=0.1 wt.%, contact time=15 min., pH=10, and ratio of ZnO/SiO₂ nanocomposite= 3:1. It is obvious that, by increasing hydrogen sulfide concentration from 100 to about 450 ppm (in constant nanoparticle concentration), the removal of hydrogen sulfide is increased. Because of the ratio of nanoparticle active site to hydrogen sulfide concentration is high. But by increasing from 450 to 800, this ratio is low; therefore, removal of hydrogen sulfide is decreased. It is noteworthy that, maximum hydrogen sulfide removal at 800 ppm of hydrogen sulfide is about 91%.

The pH with a p-value less than 0.05 is the third effective quantitative variable in hydrogen sulfide removal. Removal have a dependence on pH of drilling fluid. Fig. 6-c shows the effect of pH on removal of hydrogen sulfide from drilling fluid at condition of nanoparticle concentration= 0.1 wt.%, hydrogen sulfide concentration= 800 ppm, contact time=15 min., and ratio of ZnO/SiO₂ nanocomposite= 3:1. In the pH ranging from 8 to 12 and certain amount of hydrogen sulfide, zinc(II) can be in the forms of ZnO and ZnS. As reported previously, with the increase of pH from 8 to 12 the affinity of Zn (II) to bond with S is more favorable than the OH (Ma et al. 2013). Indeed, formation of ZnS at this pH range can favourable the adsorption of hydrogen sulfide. However, the negative surface charge of silica nanoparticle at pH 8-12 (pH_{pzc} is about 2)(Puddu and Perry 2012) is not suitable for attraction of hydrogen sulfide from drilling fluid. For ZnO/SiO₂ nanocomposite with ratio of 3:1 (Fig. 6-c), the effect of zinc oxide nanoparticle is more than silica nanoparticle. Therefore, with increase of pH, hydrogen sulfide removal from drilling fluid increases. The last quantitative variable which considered in hydrogen sulfide removal is contact time. Basically, in a removal process, the contact time is known as an equilibrium parameter. It means, at first, removal

increase by increasing contact time and then by enhancing more contact time, removal remains constant and no change. Therefore, the optimum contact time is found in order not to waste time and energy. However, according to the obtained results from Table 6 and Fig. 6-d (at condition of nanoparticle concentration= 0.1 wt.%, hydrogen sulfide concentration= 800 ppm, pH=10, and ratio of ZnO/SiO₂ nanocomposite= 3:1), contact time parameter has no effect on hydrogen sulfide removal that it is obvious that this removal process is the fast rate. So that, removal of hydrogen sulfide from drilling fluid was about 93% (93.25 to 93.9%) from 3 to 30 min.

Fig. 6-e shows the effects of ratio of ZnO/SiO₂ nanocomposite on hydrogen sulfide removal at condition of nanoparticle concentration=0.1 wt.%, hydrogen sulfide concentration= 800 ppm, pH=10, and contact time = 15 min. It is observed, the maximum hydrogen sulfide removal has for ZnO/SiO₂ nanocomposite with 3:1 ratio which is 96% at all range of nanomaterial concentration, initial hydrogen sulfide concentration, pH and contact time. The reason can be related to specific surface area and active site, so that, this nanocomposite has a maximum surface area, 208.82 m²/gr (BET analysis, Table 5) in comparison with other synthesized nanoparticle and nanocomposite.

Fig. 6

- Interaction between parameter on hydrogen sulfide removal

The interaction between hydrogen sulfide concentration and nanocomposite ratio (1:0, 0:1, 1:3, 1:1 and 3:1) are the first effective interaction on removal hydrogen sulfide from water based drilling fluid. Fig. 7-a shows the effect of interaction between two mentioned parameters at condition of nanoparticle concentration= 0.1 wt.%, contact time= 15 min., and pH=10. By increase in hydrogen sulfide from 100 to 800 ppm, ratio of active site to hydrogen sulfide in silica nanoparticle decrease and the form of ZnS to ZnO in zinc oxide nanoparticle increase. Therefore, removal of hydrogen sulfide with silica nanoparticle decrease and with zinc oxide nanoparticle increase. Also, the effect of zinc oxide nanoparticle is more prominent than the silica nanoparticle. But in nanocomposite, with increasing ratio of nanocomposite from 1:3 to 3:1, by increase in ZnO nanoparticle and surface area, removal of hydrogen sulfide increase.

The interaction between ratio of nanocomposite and pH is second effective interaction removal of hydrogen sulfide. According to Fig. 7-b (at condition of nanoparticle concentration= 0.1 wt.%, hydrogen sulfide= 400 ppm, and contact time= 15min.), that shows the effect of interaction between two mentioned parameters, in minimum and maximum hydrogen sulfide concentration (100 and 800 ppm), by increase in nanoparticle concentration from 0.1 to 0.9 wt.% for all of ratio of nanocomposite, ratio of nanoparticle active site to hydrogen sulfide increases and as a

results removal of hydrogen sulfide enhances. It is noteworthy that enhancing removal is supposed to be all of condition.

The third effective interaction is related to the nanocomposite ratio and nanoparticle concentration. Fig. 7-c demonstrates the effect of interaction between two mention parameter on removal at condition of hydrogen sulfide concentration= 400 ppm, contact time=15 min., and pH=10. It is obvious that, for all of ZnO/SiO₂ nanocomposite ratios (1:0,0:1, 1:1, 3:1 and 3:1), by increasing nanoparticle concentration, removal of hydrogen sulfide increase. The maximum removal (at all nanoparticle concentration) is dedicated to the nanocomposite with ratio of 3:1, because of the highest specific surface area in comparison with other synthesized nanomaterial. So that, the removal in 0.1 wt.% of this nanocomposite is about 93%, while removal increases to about 98% when nanocomposite concentration incremented to 0.9 wt.% in drilling fluid.

Fig. 7

3.3. Optimum condition for hydrogen sulfide removal from drilling fluid

One of the other benefits of using Design Expert software is the software ability to determine the removal optimum condition by selecting and adjusting of the conditions. The economic considerations in nanomaterial utilization are so important at removal of hydrogen sulfide from drilling fluid, therefore the optimum condition was investigated by the maximum and minimum nanoparticle concentration (0.1 and 0.9 wt.%), maximum hydrogen sulfide concentration (800 ppm), minimum contact time (5 min.) and pH in rage of 8 to 12. Fig. 8 shows the results of removal of hydrogen sulfide from drilling fluid in optimum condition. Consider to the highest removal in the maximum and the minimum nanoparticle concentration are 97.2% (with desirability of 0.98) and 92.6% (with desirability of 0.941) that, the difference between these removals is 4.6%. Therefore, the best concentration (point of economic) of nanocomposite for removal of hydrogen sulfide is 0.1 wt.% (minimum concentration) of ZnO/SiO₂ nanocomposite with ratio of 3:1. This optimum condition was done in the same condition in Drilling nanofluid laboratory and the obtained removal was 91.25 and 96 %.

Fig. 8

3.4. kinetic study

In order to kinetic describe of hydrogen sulfide removal by ZnO, SiO₂ nanoparticle and ZnO/SiO₂ nanocomposite from drilling fluid, two models of the pseudo-first order (Eq. 2) (Lagergren 1898) and pseudo-second order (Eq. 3) (Ho and McKay 1999) are presented. Two model are linearized and are fitted with experimental data.

$$\ln(q_e - q_t) = -k_1 t + \ln q_e \quad (2)$$

$$\frac{t}{q_t} = \frac{1}{k_2 q_e^2} + \frac{t}{q_e} \quad (3)$$

Where K_1 (min^{-1}) and K_2 ($\text{g mg}^{-1}\text{min}^{-1}$) are rate constant of pseudo-first order and pseudo- second order that are obtaining from slope of Fig. $-\ln(q_e-q_t)$ versus contact time and Fig. $\frac{q_t}{t}$ versus contact time, respectively. q_e and q_t (mg g^{-1}) are adsorption capacity in balance time (equilibrium) and in contact time t . Also, the following formula (Eq. 4) can be used in order to calculate q_t :

$$q_t = \frac{(c_0 - c_e)V}{m} \quad (4)$$

Where c_0 and c_e (mg L^{-1}) are initial and secondary (at t) concentration of hydrogen sulfide in drilling fluid; V is a sample volume with a unit of (ml); and m is nanoparticle concentration (mg).The regression results for pseudo- first and second order are showed in Fig. 9-a and b and Table 7. Correlation coefficient values (R^2) for pseudo-first order (0.971) is more than pseudo-second order (0.936). Therefore, the pseudo-first order is suggested for removal hydrogen sulfide from drilling fluid.

It is noteworthy that the amount of obtained constant rate from peseudo-first order is so more compare to other constant rates, are reported in related reference, which this subject conforms to high removal rate of hydrogen sulfide and contact time interval (3 to 30 min.) has no significant effect on hydrogen sulfide removal.

Fig. 9

Table 7

In order to investigate the adsorption mechanism (monolayer or multilayer and physical or chemical adsorption) of hydrogen sulfide from water based drilling fluid, two isotherm models, Langmuir and Freundlich are used (Gessner and Hasan 1987; Achife and Ibemesi 1989). On Langmuir model, it is assumed that hydrogen sulfide covers on nanoparticle only in a monolayer (chemical adsorption) form and all adsorption sites are identical base on energy and enthalpy level. The linear form of Langmuir model (Eq. 5) express as follow:

$$\frac{C_e}{q_e} = \frac{1}{q_m K_L} + \frac{C_e}{q_m} \quad (5)$$

Where q_e is adsorption balance capacity, C_e is hydrogen sulfide balance concentration (mg L^{-1}), K_L (L mg^{-1}) is Langmuir balance constant, and a_L is Langmuir adsorption enthalpy constant. According to Langmuir equation, the maximum of adsorption (mg g^{-1}) can be calculated by the following equation (Eq. 6):

$$q_m = \frac{K_L}{a_L} \quad (6)$$

On C can be used for multisite adsorption (chemical adsorption) with rough surfaces. Freundlich adsorption model is obtaining by adding assumption of logarithmic distribution of adsorption energy to Langmuir equation. This model describes a reversible adsorption. Freundlich adsorption equation (Eq. 7) is as follow:

$$q = K_f C_e^{1/n} \quad (7)$$

On this equation, q and C_e are the same as Langmuir equation. K_f and n are Freundlich constants that K_f is an index for adsorption capacity, and n is an experimental constant. According to the following equation, Freundlich equation constants are calculating from Fig of $\log q$ versus $\log C_e$. The linear form of Freundlich equation (Eq. 8) is as follow:

$$\log q = \log K_f + \left(\frac{1}{n}\right) \log C_e \quad (8)$$

The regression results of comparing the experimental data to Langmuir and Freundlich models are indicated in Fig. 10. Also, Table 8 illustrates the calculated adsorption parameters of isothermal curves of Freundlich and Langmuir adsorption. The correlation coefficient comparison of these models shows that Freundlich model ($R^2=0.997$) is better matching to experimental data. Therefore, adsorption of hydrogen sulfide on nanocomposite occurs in a multilayer form.

Fig. 10

Table 8

3.5. Reusability of nanomaterial

In order to study the reusability of synthesized nanoparticle and nanocomposite with and without washing, by applying the optimum conditions including Initial hydrogen sulfide concentration, 800 ppm, and ZnO/SiO₂ nanocomposite with ratio of 3:1, nanocomposite concentration, 0.1 and 0.9 wt.%, pH, 12, and contact time, 3 min., nanocomposite was added to drilling fluid (with hydrogen sulfide) for several times, that the results are showed in Fig. 11-a and b. It is obvious that, ZnO/SiO₂ nanocomposite with minimum and maximum concentration with and

without washing by deionized water for at least four cycles in hydrogen sulfide removal with adsorption efficiency of more than 50% is acceptable. It is noteworthy that, reusability and removal efficiency for nanocomposite with washing process is better than without washing by deionized water.

Fig. 11

4. Conclusion

In order to removal hydrogen sulfide from drilling fluid, ZnO and SiO₂ nanoparticles and ZnO/SiO₂ nanocomposite with different ratio were synthesized by precipitation and sol-gel method and characterized. The Design Expert software, I-optimal method, was used to design the experiments and obtained optimum condition (0.1 and 0.9 wt.%, 800 ppm, 3 min and pH=12). The maximum removal in the optimum conditions was 92.6% and 97.2% at minimum and maximum nanoparticle concentration. Moreover, the investigation of kinetic and isotherm of adsorption revealed that the removal process follows pseudo-second order, Freundlich isothermal and multisite adsorption model. This nanoparticle has the ability to be used at least in four cycles consecutive hydrogen sulfide removal with efficiency of greater than 50% and the reusability for washing nanocomposite is better than without washing. Also, hydrogen sulfide removal is significantly fast and contact time has a few impact on the process.

References

- Achife E, Ibemesi J. Applicability of the Freundlich and Langmuir adsorption isotherms in the bleaching of rubber and melon seed oils. *J of the Ame Oil Chem Soc.* 1989; 66(2): 247-252.
- Ali A, Harraz MFA, Ismail AA, et al. Synthesis of amorphous ZnO–SiO₂ nanocomposite with enhanced chemical sensing properties. *Thin Solid Films.* 2016; 605:277-282.
- Arshad A, Farrukh MA, Ali S, et al. Development of Latent Fingermarks on Various Surfaces Using ZnO- SiO₂ Nanopowder. *J of forensic sci.* 2015; 60(5):1182-1187.
- Awume B, Tajallipour M, Nemati M, et al. Application of ZnO Nanoparticles in Control of H₂ S Emission from Low-Temperature Gases and Swine Manure Gas. *Water, Air, & Soil Pollution.* 2017; 228(4):147.
- Bagheri S, Chandrappa K, Hamid SBA. Facile synthesis of nano-sized ZnO by direct precipitation method. *Der Pharma Chemica.* 2013; 5(3):265-270.
- Blatt, O, Helmich M, Steuten B, et al. Iron Oxide/Polymer- Based Nanocomposite Material for Hydrogen Sulfide Adsorption Applications. *Chem Eng Tech* 2014; 37(11):1938-1944.

Carney LL, Jones B. Practical Solutions to Combat the Detrimental Effects of Hydrogen Sulfide During Drilling Operations. SPE Symposium on Sour Gas and Crude, Society of Petroleum Engineers.1974.

Daneshyar A, Ghaedi M, Sabzehmeidani M. H₂S adsorption onto Cu-Zn-Ni nanoparticles loaded activated carbon and Ni-Co nanoparticles loaded γ -Al₂O₃: optimization and adsorption isotherms. J of colloid and interf sci 2017; 490:553-561.

Dargahi-Zaboli M, Sahraei E, Pourabbas B. Hydrophobic silica nanoparticle-stabilized invert emulsion as drilling fluid for deep drilling. Pet Sci. 2017; 14(1):105-115.

Esmaeili-Faraj SH, Nasr Esfahany M. Absorption of hydrogen sulfide and carbon dioxide in water based nanofluids. Ind Eng Chem Res. 2016; 55(16):4682-4690.

Fauteux-Lefebvre C, Abatzoglou N, Braidy N, et al. Carbon nanofilaments functionalized with iron oxide nanoparticles for in-depth hydrogen sulfide adsorption. Industrial & Eng Chem Res. 2015; 54(37):9230-9237.

Gessner, PK, Hasan MM, Freundlich and Langmuir isotherms as models for the adsorption of toxicants on activated charcoal. J of pharm sci. 1987; 76(4):319-327.

Goldstein JI, Newbury DE, Michael JR, et al. Scanning electron microscopy and X-ray microanalysis. 4rd ed. Springer; 2017.

Han CH, Han SD, Khatkar S. Enhancement of H₂-sensing properties of F-doped SnO₂ sensor by surface modification with SiO₂. Sensors. 2006; 6(5):492-502.

Hasnidawani J, Azlina H. Norita H, et al. Synthesis of ZnO nanostructures using sol-gel method. Procedia Chem. 2016; 19:211-216.

HoYS, McKay G. Pseudo-second order model for sorption processes. Process biochem. 1999; 34(5):451-465.

Jurablu S, Farahmandjou M, Firoozabadi T. Sol-Gel Synthesis of Zinc Oxide (ZnO) Nanoparticles: Study of Structural and Optical Properties. J of Sci, Islamic Republic of Iran. 2015; 26(3):281-285.

Kumar SS, Venkateswarlu P, Rao VR, et al. Synthesis, characterization and optical properties of zinc oxide nanoparticles. Inter Nano Letters. 2013; 3(1):1-30.

Lagergren SK. About the theory of so-called adsorption of soluble substances. Sven. Vetenskapsakad. Handlingar. 1898; 24:1-39.

Lim SK, Hwang SH, Kim S. Preparation of ZnO nanorods by microemulsion synthesis and their application as a CO gas sensor. Sensors and Actuators B: Chemical. 2011; 160(1):94-98.

Liu C, Zhang R, Wei S, et al. Selective removal of H₂S from biogas using a regenerable hybrid TiO₂/zeolite composite. *Fuel*. 2015; 157: 183-190.

Liu G, Huang ZH, Kang F. Preparation of ZnO/SiO₂ gel composites and their performance of H₂S removal at room temperature. *J of hazardous materials*. 2012; 215:166-172.

Ma R, Levard C, Michel FM, et al. Sulfidation Mechanism for Zinc Oxide Nanoparticles and the Effect of Sulfidation on Their Solubility. *Environ Sci Technol*. 2013; 47:2527–2534.

Ma M, Zou C. Enhancement by SiC Nanoparticles of the Removal of Hydrogen Sulfide from Natural Gas by a Traditional Desulfurizer. *Energy & Fuels*. 2017; 31(8):8054-8060.

Morgani MS, Saboori R, Sabbaghi S. Hydrogen sulfide removal in water-based drilling fluid by metal oxide nanoparticle and ZnO/TiO₂ nanocomposite. *Mat Res Exp*. 2017; 4(7):075501.

Musić S, Filipović-Vinceković N, Sekovanić L. Precipitation of amorphous SiO₂ particles and their properties. *Bra J of chem Eng*. 2011; 28(1):89-94.

PudduV, Perry CC. Peptide adsorption on silica nanoparticles: evidence of hydrophobic interactions. *ACS nano*. 2012; 6(7):6356-6363.

Raevskaya A, Panasiuk YV, Stroyuk O, et al. Spectral and luminescent properties of ZnO-SiO₂ core-shell nanoparticles with size-selected ZnO cores. *RSC Adv*. 2014; 4(108):63393-63401.

Rahman IA, Padavettan V. Synthesis of silica nanoparticles by sol-gel: size-dependent properties, surface modification, and applications in silica-polymer nanocomposites-a review. *J of Nanomaterials*. 2012; 2012:1-8.

Saboori R, Azin R, Osfoury et al. Wettability alteration of carbonate rocks from strongly liquid-wetting to strongly gas-wetting by fluorine-doped silica coated by fluorosilane. *J of Disp Sci and Tech*. 2018; 39(6):767-776.

Saboori R, Sabbaghi S, Kalantariasl A, et al. Improvement in filtration properties of water-based drilling fluid by nanocarboxymethyl cellulose/polystyrene core-shell nanocomposite. *J of Petr Exp and Prod Tech*. 2018; 1-10.

Sekhvatjou MS, Moradi R, Hosseini Alhashemi A, et al. A new method for sulfur components removal from sour gas through application of zinc and iron oxides nanoparticles. *Int J of Envi Res*. 2014; 8(2):273-278.

Shastri L, Qureshi M, Malik M. Photoluminescence study of ZnO-SiO₂ nanostructures grown in silica matrix obtained via sol-gel method. *J of Phy and Chem of Solids*. 2013; 74(4):595-598.

Skoog DA, Holler FJ, Crouch SR. *Principles of instrumental analysis*. Cengage learning; 2017.

Speakman SA. Estimating crystallite size using XRD. MIT Center for Mat Sci and Eng. 2014.

Stöber W, Fink A, Bohn E. Controlled growth of monodisperse silica spheres in the micron size range. *J of colloid and interf sci.* 1968; 26(1):62-69.

Sunde E, Olsen H. Removal of H₂S in drilling mud. 1999.

Wang X, Sun T, Yang J, et al. Low-temperature H₂S removal from gas streams with SBA-15 supported ZnO nanoparticles. *Chem Eng J.* 2008; 142(1):48-55.

Zhang Z, Liu B, Wang F, et al. Hydrogen sulfide removal from hot coal gas by various mesoporous silica supported Mn₂O₃ sorbents. *Appl Surf Sci.* 2014; 313:961-969.

Figure Captions:

Fig. 1 Procedure of ZnO/SiO₂ nanocomposite synthesis with 1:1 ratio.

Fig. 2 The XRD pattern of; (a) ZnO nanoparticle, (b) SiO₂ nanoparticle, (c) ZnO/SiO₂ nanocomposite with a ratio of 1:1, (d) ZnO/SiO₂ nanocomposite with a ratio of 3:1, and (e) ZnO/SiO₂ nanocomposite with a ratio of 1:3.

Fig. 3 EDAX analysis of ZnO/SiO₂ nanocomposite with a ratio of 1:3, 1:1, and 3:1.

Fig. 4 FT-IR analysis of the, (a) ZnO nanoparticle, (b) SiO₂ nanoparticle, and (c) ZnO/SiO₂ nanocomposite for different ratio: (a) 3:1, (b) 1:3, and (c) 1:1.

Fig. 5 FE-SEM image of (a) ZnO nanoparticle, (b) SiO₂ nanoparticles, (c) ZnO/SiO₂ nanocomposite with ratio of 1:1, (d) ZnO/SiO₂ nanocomposite with ratio of 1:3, and (e) ZnO/SiO₂ nanocomposite with ratio of 3:1.

Fig. 6 The Effect of (a) nanoparticle concentration, (b) hydrogen sulfide concentration, (c) pH, (d) contact time, and (e) nanocomposite ratio on hydrogen sulfide removal from drilling fluid.

Fig. 7 The effect of interaction between (a) hydrogen sulfide concentration and ratio of nanocomposite, (b) ratio of nanocomposite and pH, and (c) hydrogen nanoparticle concentration and ratio of nanocomposite on removal from drilling fluid.

Fig. 8 Optimum condition for hydrogen sulfide removal from drilling fluid, a) minimum nanoparticle concentration, and b) maximum nanoparticle concentration.

Fig. 9 The result of kinetic study of hydrogen sulfide adsorption from drilling fluid (a)The pseudo-first order and (b) the pseudo-second order.

Fig. 10 The isothermal curves for hydrogen sulfide adsorption from drilling fluid with ZnO/SiO₂ nanocomposite, (a) Freundlich model and (b) Langmuir model.

Fig. 11 The reusability of nanomaterial at optimum condition: (a) Maximum nanomaterial concentration (0.1 wt.%), and (b) minimum nanomaterial concentration (0.9 wt.%).

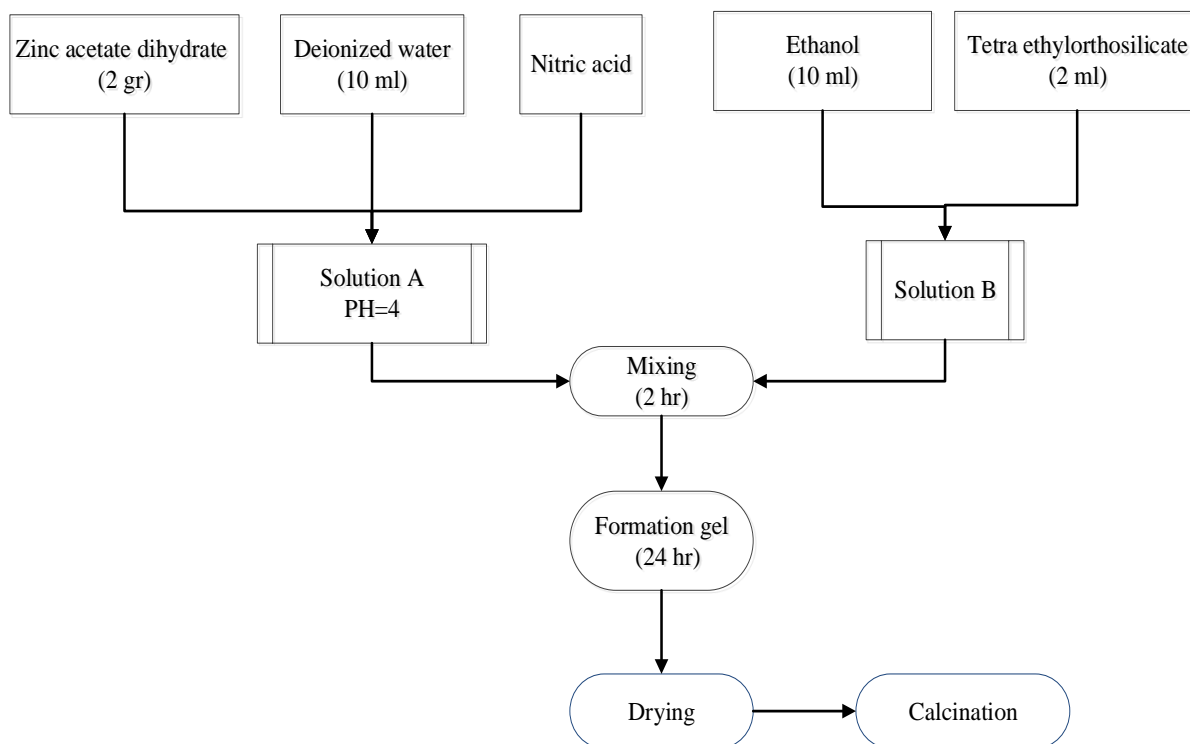
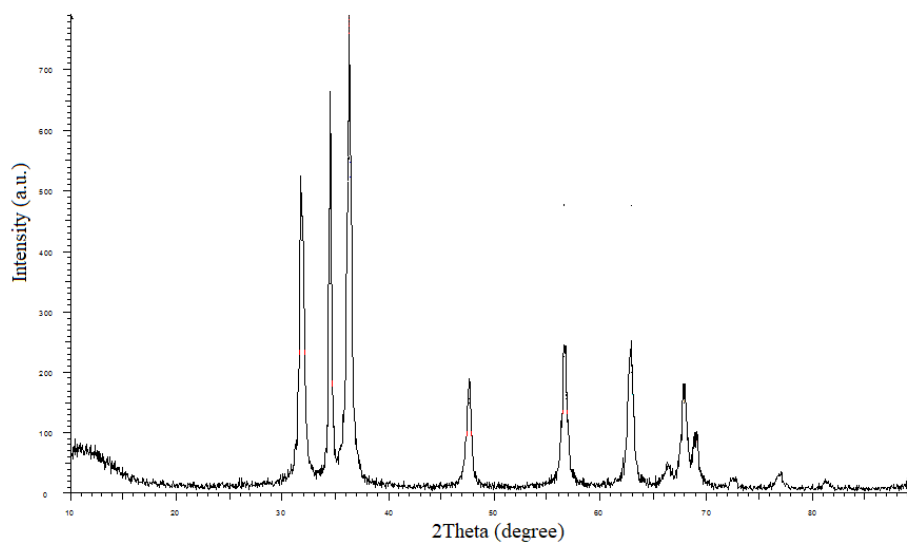
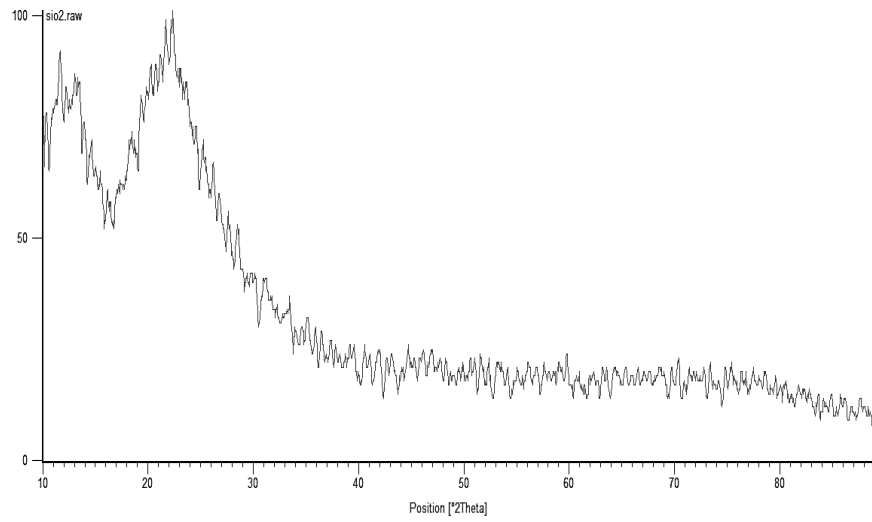


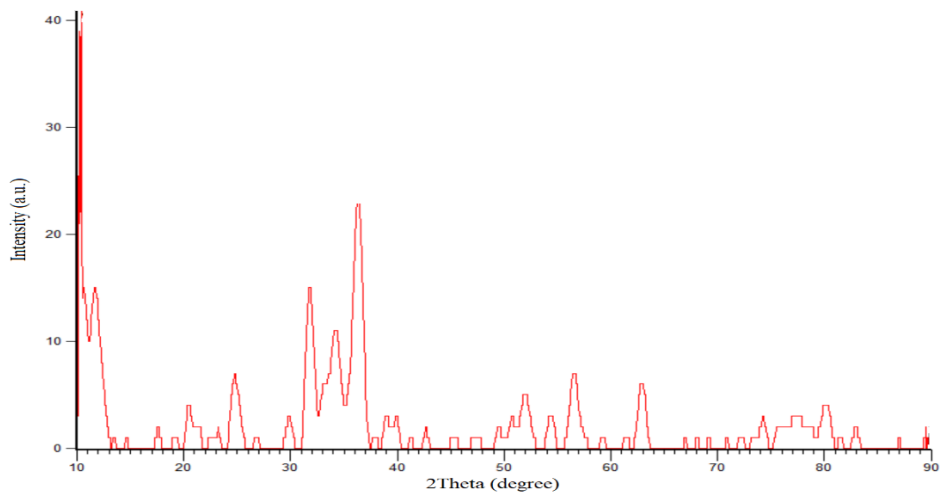
Fig. 1



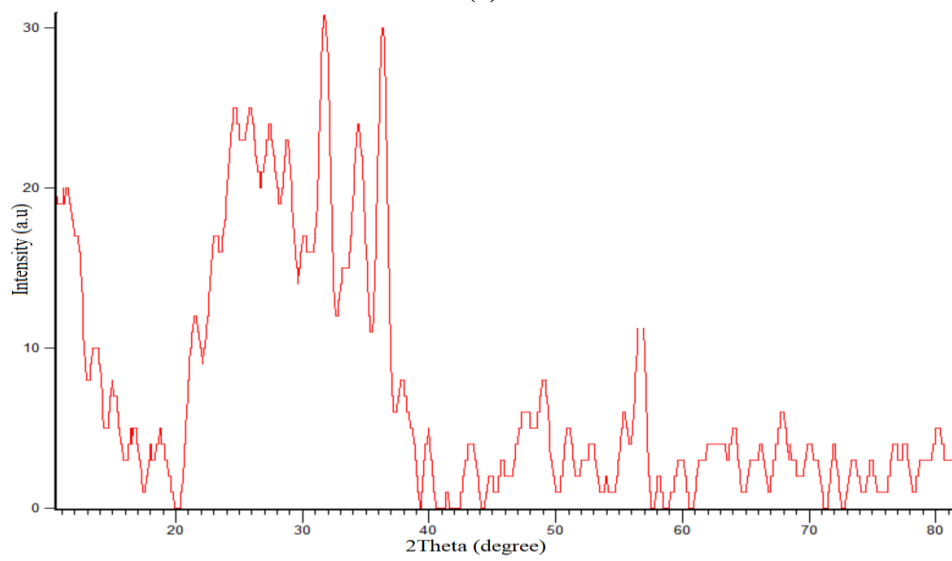
(a)



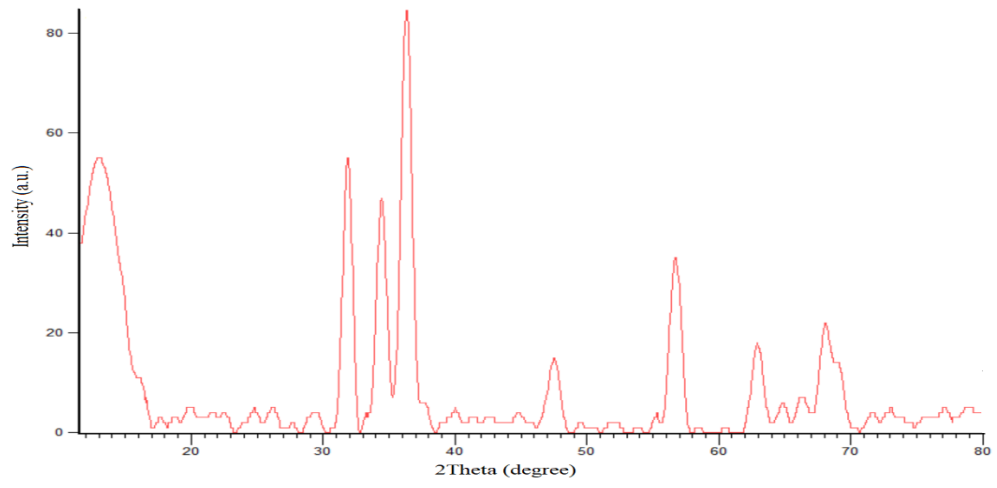
(b)



(c)



(d)



(e)
Fig. 2

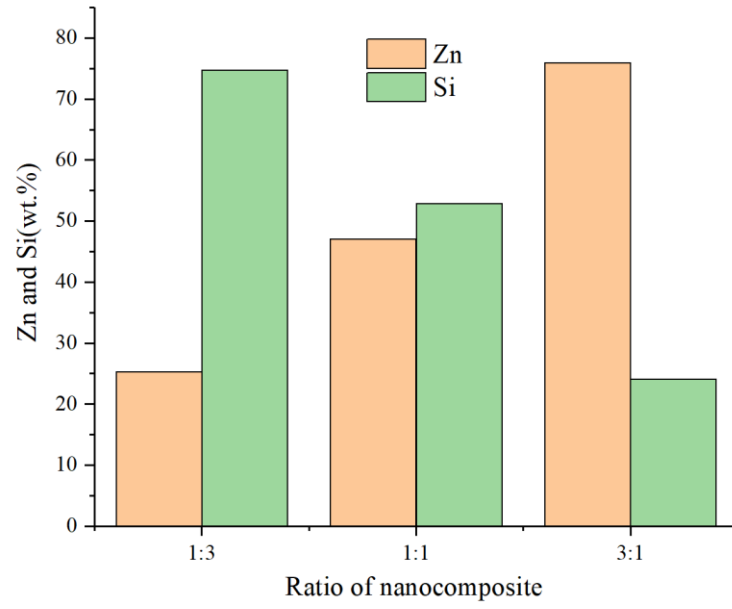
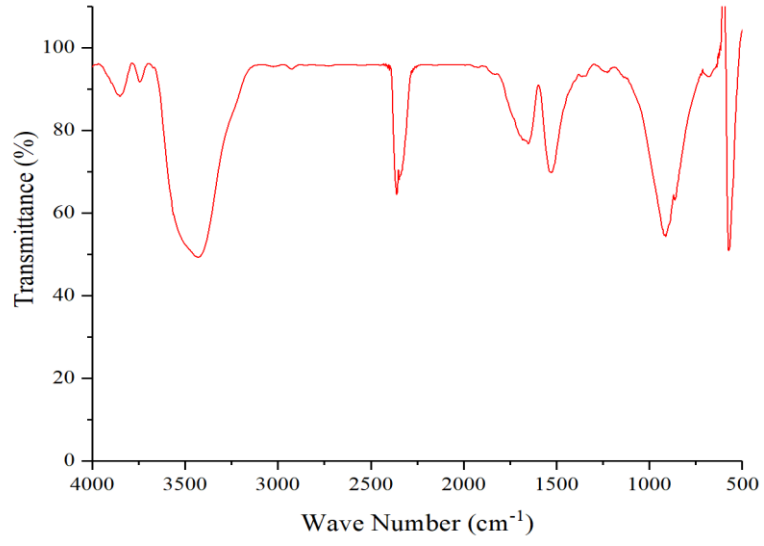
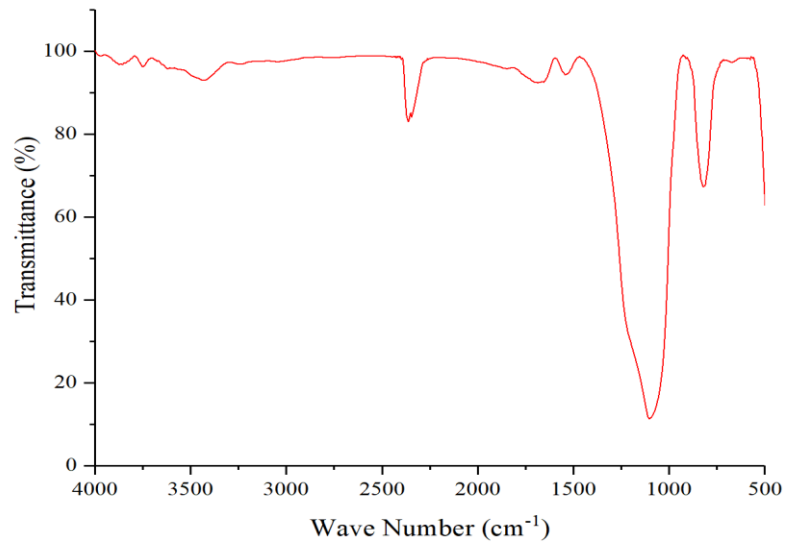


Fig. 3



(a)



(b)

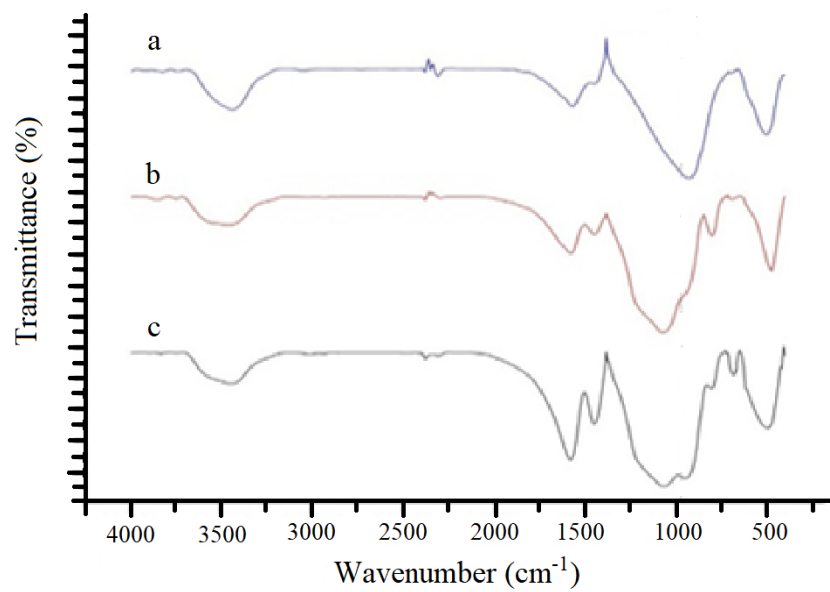
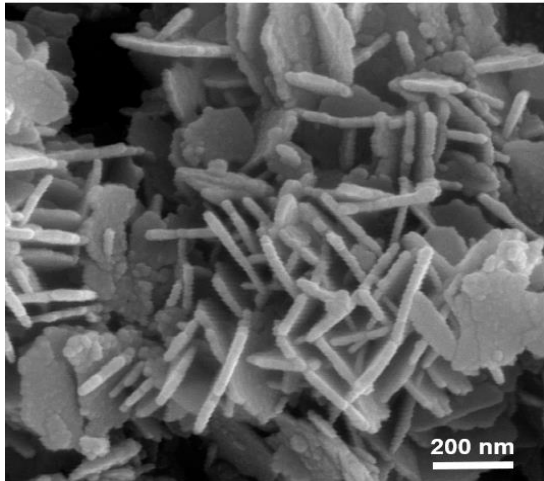
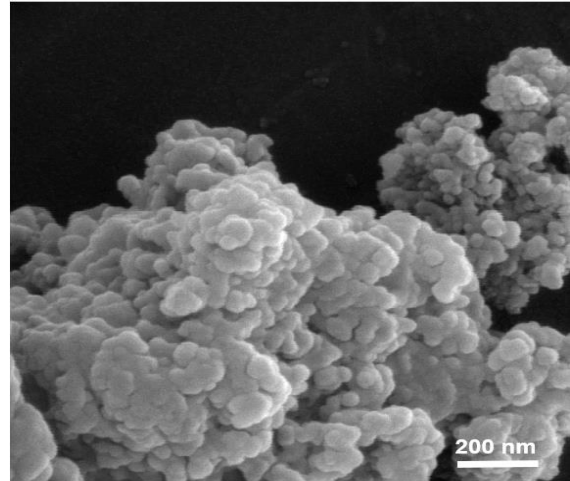


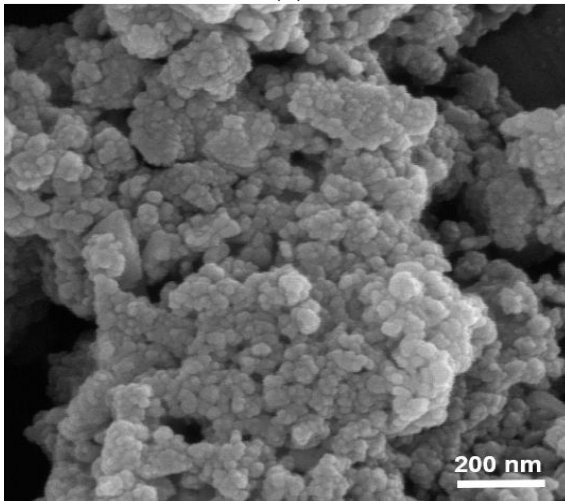
Fig. 4



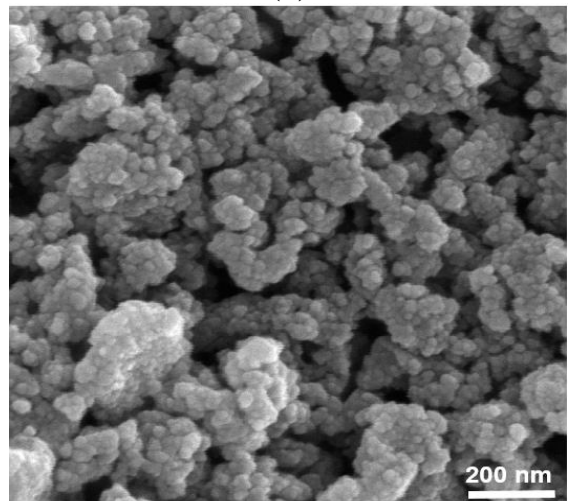
(a)



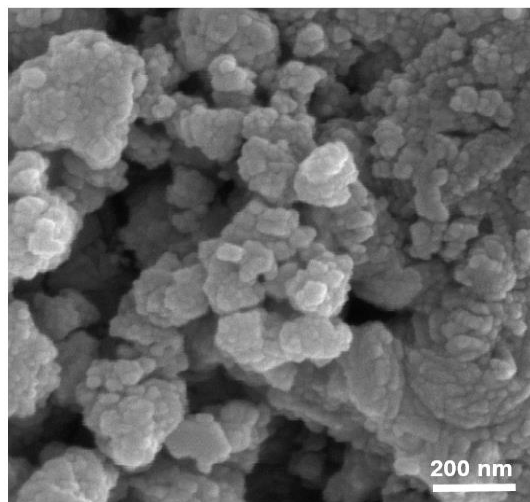
(b)



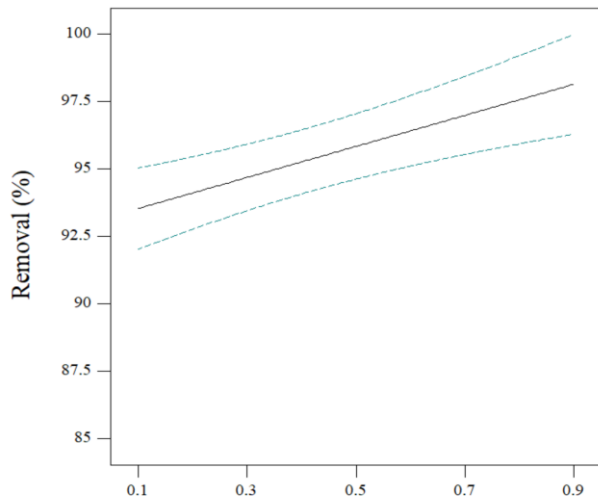
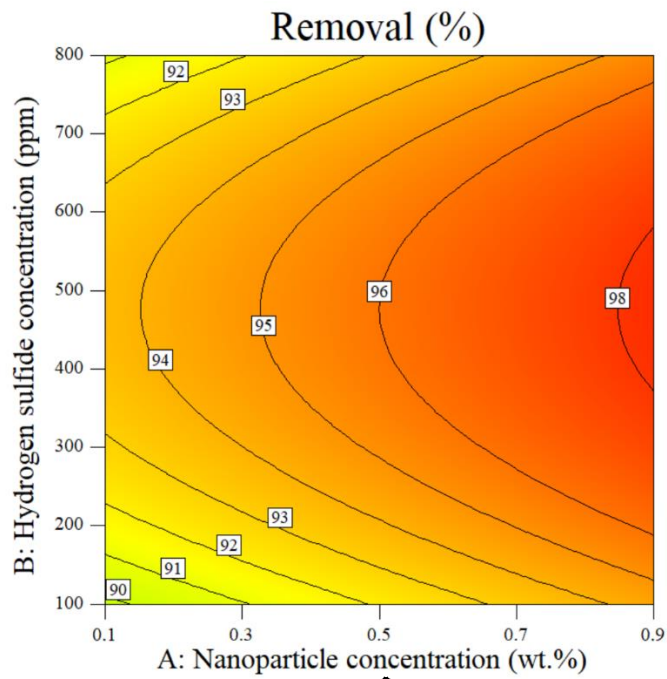
(c)



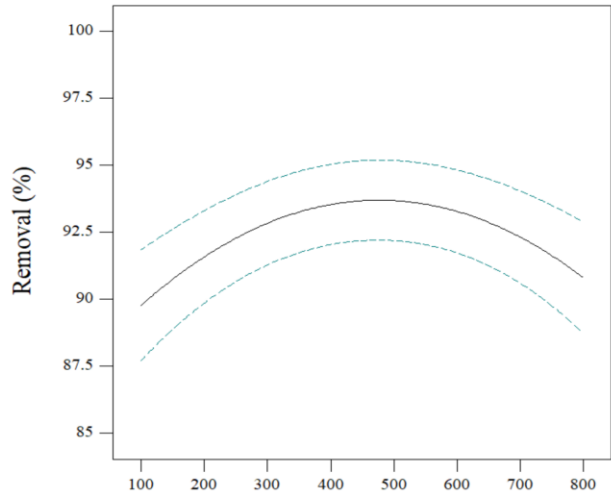
(d)



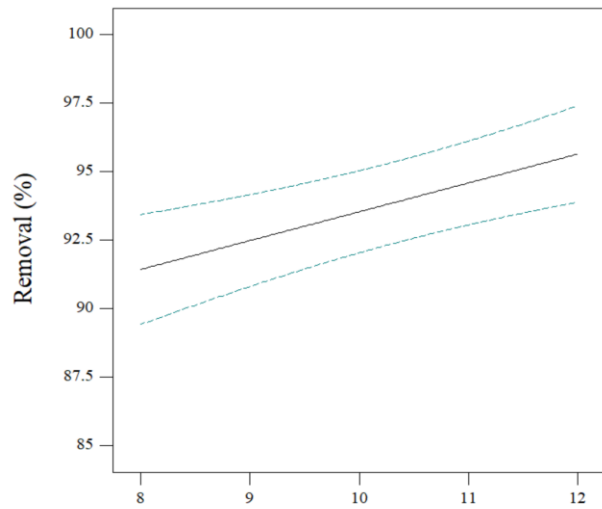
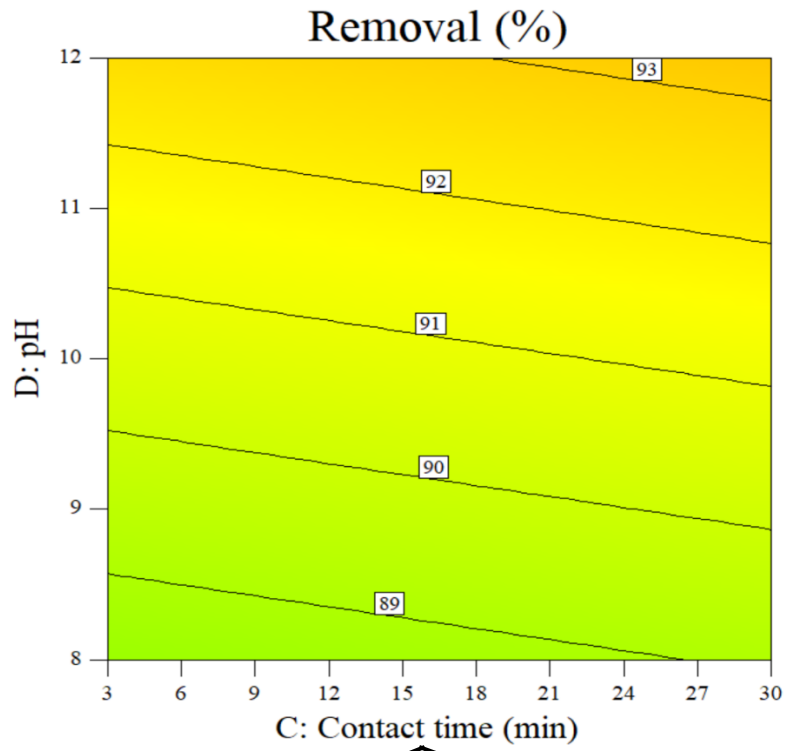
(e)
Fig. 5



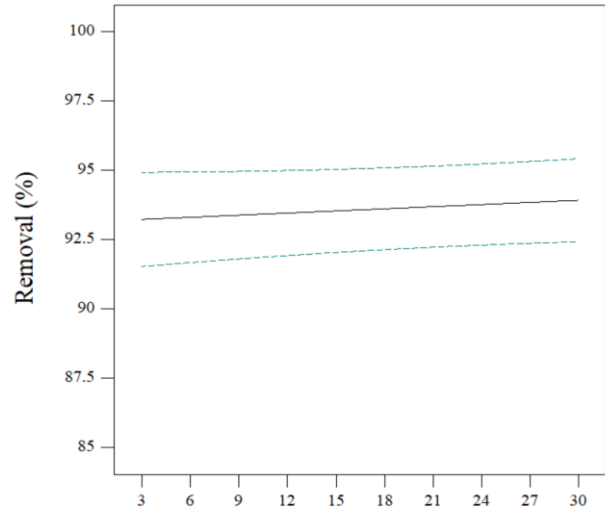
(a)



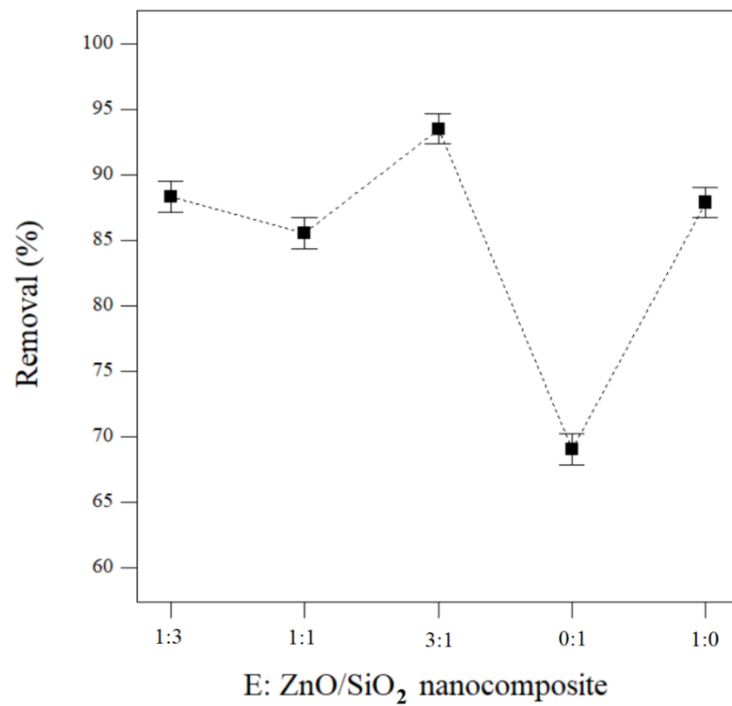
(b)



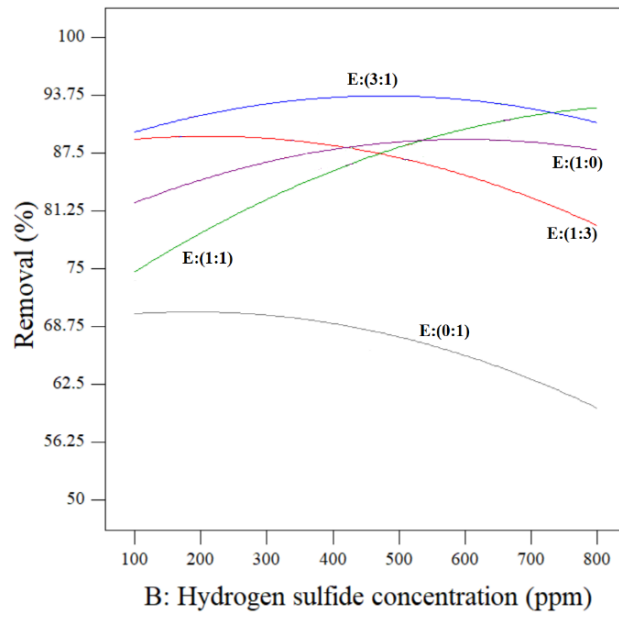
D: pH
(c)



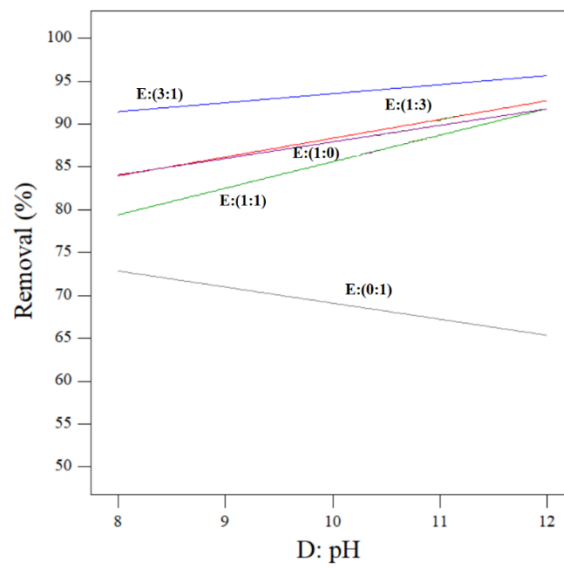
C: Contact time (min)
(d)



(e)
Fig. 6



(a)



(b)

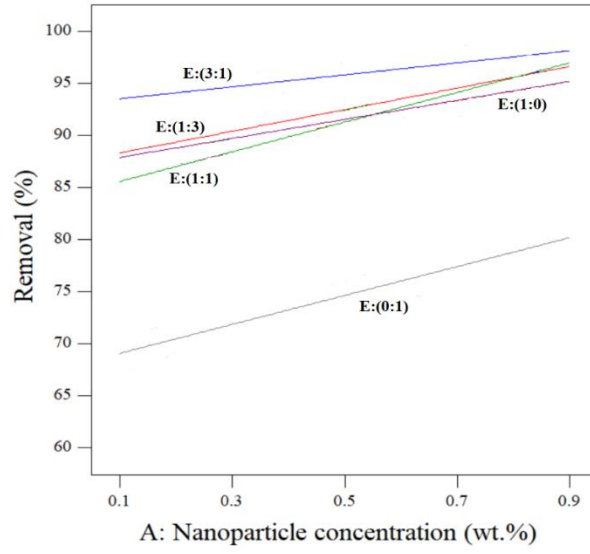
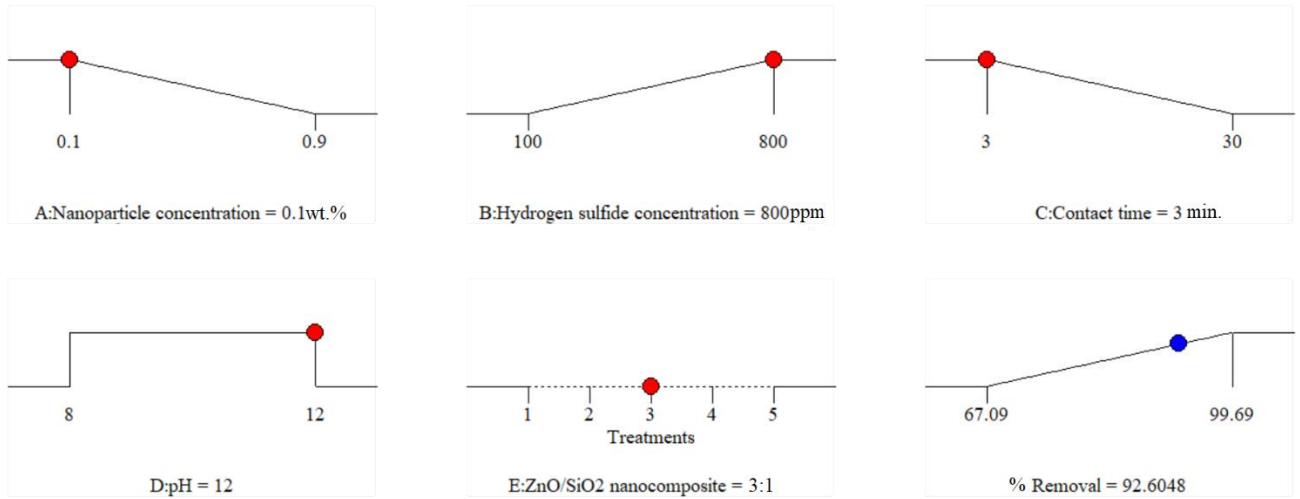
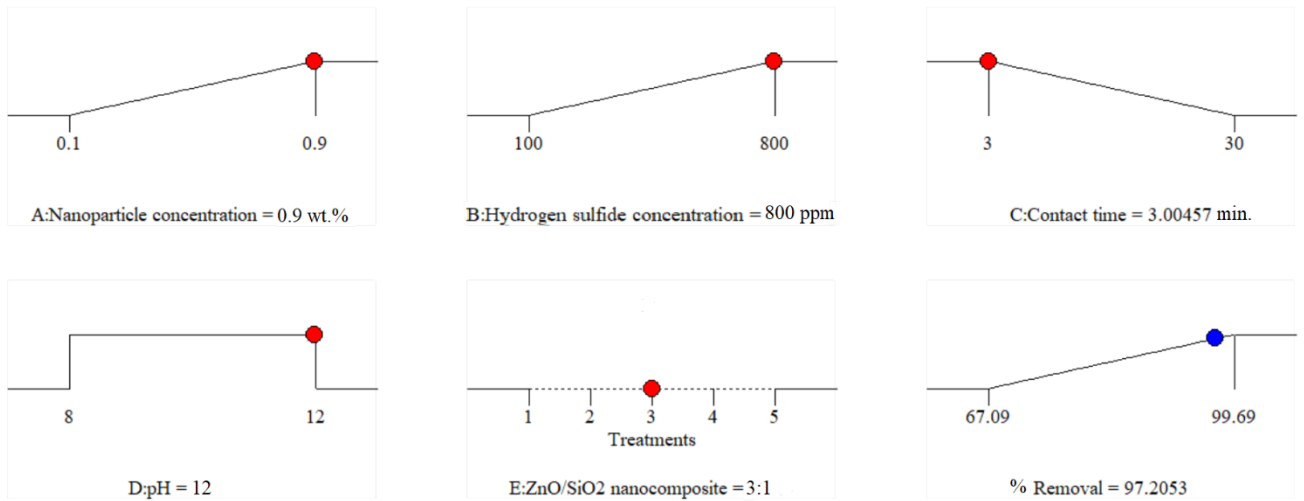


Fig. 7



Desirability = 0.941

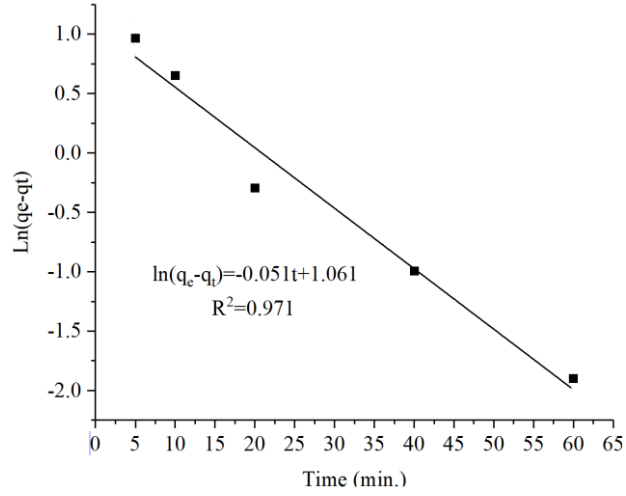
(a)



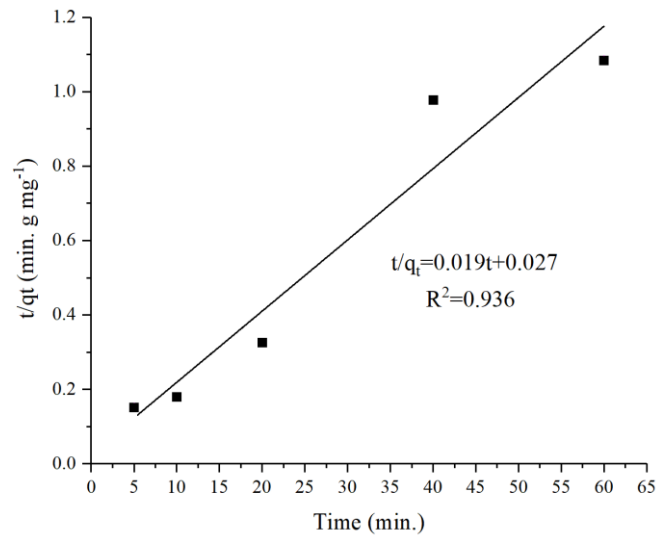
Desirability = 0.980

(b)

Fig. 8

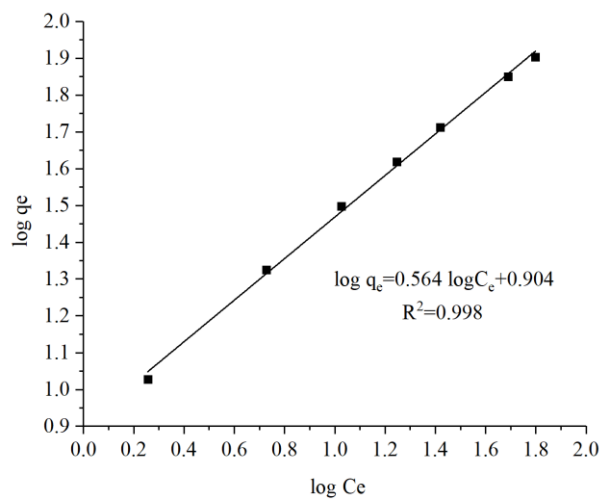


(a)

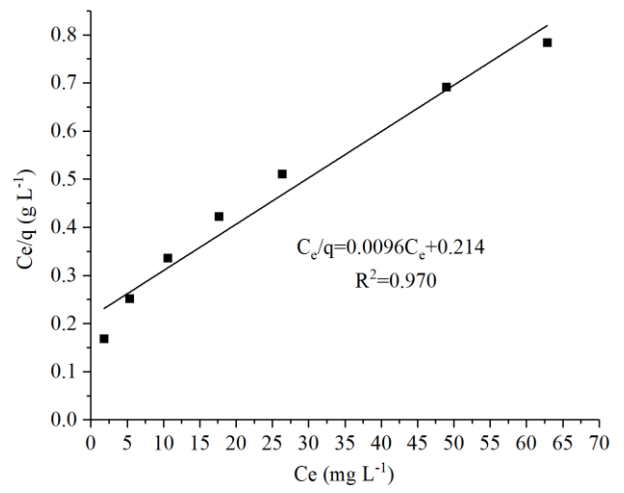


(b)

Fig. 9



(a)



(b)

Fig. 10

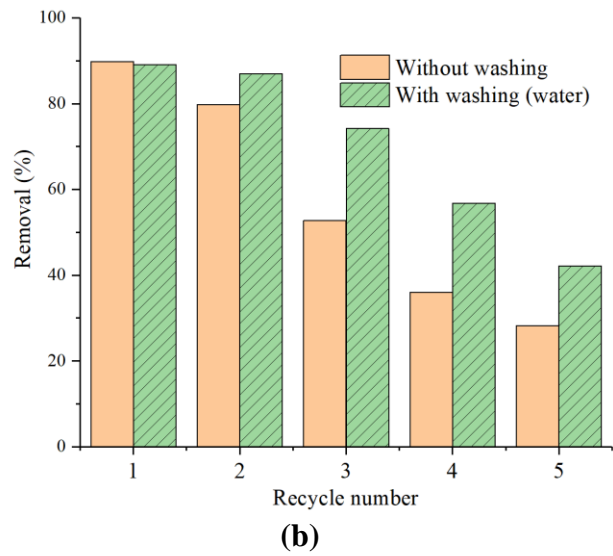
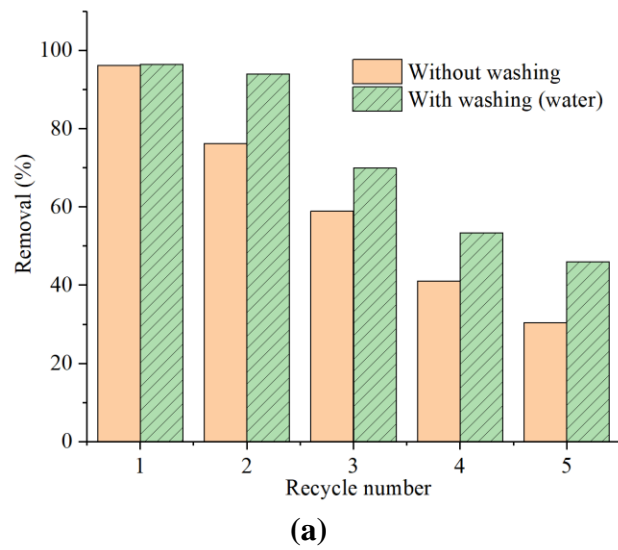


Fig. 11

Table Captions:

Table 1: Amount of materials for nanocomposite synthesis with different ratio.

Table 2: The effective parameter and their range on hydrogen sulfide removal from water based drilling fluid.

Table 3: The crystallite size of the synthesized nanoparticles and the nanocomposites.

Table 4: Specific surface area for synthesized nanoparticle.

Table 5: The designed experiments with Design Expert software and their results.

Table 6: Variance analysis.

Table 7: Calculated parameter for two kinetic models in hydrogen sulfide removal.

Table 8: The adsorption parameters of isothermal model.

Table 1:

ZnO/SiO₂ nanocomposite (molar ratio)	Zinc acetate dihydrate (gr)	Deionized water (ml)	Tetraethyl orthosilicate (ml)	Ethanol (ml)
1:1	2	10	2	10
3:1	2	10	6	15
1:3	2	10	0.3	1.5

Table 2:

Variables	Unit	range
Hydrogen sulfide concentration	mL	100-800
Nanomaterial concentration	wt. %	0.1-0.9
pH	---	8-12
Time	min.	3-30

Table 3:

Nanomaterial	K	$\lambda(\text{nm})$	β (rad.)	2θ	$\tau(\text{nm})$
ZnO	0.90	0.156	0.01029	36.27	14.20
SiO ₂	0.90	0.156	0.01029	22.25	13.58
SiO ₂ /ZnO (1:1)	0.90	0.156	0.01716	39.33	10.66
SiO ₂ /ZnO (1:3)	0.90	0.156	0.01717	36.32	8.52
SiO ₂ /ZnO (3:1)	0.90	0.156	0.01373	31.71	10.55

Table 4:

Ratio of ZnO/SiO₂ nanocomposite	Specific surface area (m²gr⁻¹)
1:0	36.18
0:1	16.39
1:1	129.72
1:3	51.62
3:1	208.82

Table 5:

Run	A	B	C	D	E	Removal (%)	Run	A	B	C	D	E	Removal (%)
1	0.9	800	5	3	3:1	88.28	2	0.7	100	5	11	1:3	80.08
3	0.5	400	5	9	3:1	80.90	4	0.7	200	30	9	0:1	76.34
5	0.1	400	10	11	1:3	56.06	6	0.9	100	30	3	1:1	82.57
7	0.3	300	20	3	1:0	68.04	8	0.5	800	20	5	1:1	65.21
9	0.3	100	30	3	1:3	62.93	10	0.9	500	20	11	1:0	83.40
11	0.5	400	5	9	3:1	85.68	12	0.5	800	5	9	1:3	60.46
13	0.5	800	20	5	1:1	68.25	14	0.5	500	30	3	3:1	77.75
15	0.9	500	3	9	1:1	82.40	16	0.1	800	20	7	3:1	65.04
17	0.1	500	10	7	1:1	60.66	18	0.5	100	20	11	1:1	76.65
19	0.7	100	3	7	1:0	80.42	20	0.9	100	20	7	3:1	96.06
21	0.7	300	20	5	0:1	75.38	22	0.3	800	20	11	1:0	60.04
23	0.1	500	30	11	1:3	56.71	24	0.3	800	3	5	0:1	56.37
25	0.1	100	3	3	3:1	67.58	26	0.1	400	30	7	1:1	62.70
27	0.9	300	3	5	3:1	91.14	28	0.9	800	20	5	0:1	78.45
29	0.7	800	30	5	1:0	70.30	30	0.1	100	30	11	1:0	68.46
31	0.9	200	20	3	1:0	80.78	32	0.1	200	10	7	0:1	61.21
33	0.1	800	30	3	0:1	49.27	34	0.1	800	3	11	1:1	60.79
35	0.9	500	20	5	1:3	75.43	36	0.1	800	5	9	1:0	58.97
37	0.9	100	3	11	0:1	88.85	38	0.7	100	5	3	0:1	73.56
39	0.9	800	30	11	3:1	92.41	40	0.1	400	3	3	1:3	51.09
41	0.1	100	30	11	3:1	73.97	42	0.3	100	5	3	1:1	67.63

A: Nanoparticle concentration (wt.%), B: Hydrogen sulfide concentration (ppm), C: Contact time (min.), D: pH, E: ratio of ZnO/SiO₂ nanocomposite.

Table 6:

Source	Sum of Squares	Mean Square	F-Value	p-value
Model	3477.21	165.58	86.70	< 0.0001
Nanoparticle concentration (A)	384.10	384.10	201.12	< 0.0001
Hydrogen sulfide concentration(B)	2.38	2.38	1.25	0.2775
Contact time (C)	2.81	2.81	1.47	0.2391
pH (D)	308.67	308.67	161.62	< 0.0001
Ratio of ZnO/SiO₂ (E)	2167.30	541.82	283.71	< 0.0001
BE	315.41	78.85	41.29	< 0.0001
DE	92.05	23.01	12.05	< 0.0001
AE	34.99	8.75	4.58	0.0087
B²	71.86	71.86	37.63	< 0.0001
R-square=0.9891	Adj R-Squared=0.9777	Pred R-Squared=0.9542		

Table 7:

Kinetic model	K₁ (min⁻¹)	K₂ (g mg⁻¹min⁻¹)	R²
Pseudo-first order	0.051	-	0.971
Pseudo-second order	-	0.013	0.936

Table 8:

Langmuir model			Freundlich model		
q_m (mg g^{-1})	K_L ($\text{mg}^{-1} \text{L}$)	R^2	n	K_F ($\text{mg}^{1-n} \text{L}^n \text{g}^{-1}$)	R^2
104.17	0.05	0.969	1.78	8.02	0.997